AIMS Mathematics, 11(1): 684–716.
DOI: 10.3934/math.2026030
Received: 03 October 2025
Revised: 12 December 2025
Accepted: 16 December 2025
Published: 09 January 2026

https://www.aimspress.com/journal/Math

Research article

Dynamical analysis of an SIR epidemic model with game-theoretic vaccination behavior

Fengjun Li[1,*], Tao Zhang[2] and Qimin Zhang[2]

[1] School of Mathematics and Information Science, North Minzu University, Yinchuan, Ningxia 750021, China

[2] School of Mathematics and Statistics, Ningxia University, Yinchuan, Ningxia 750021, China

* **Correspondence:** Email: fjli@nmu.edu.cn.

Abstract: In this paper, a susceptible–infectious–recovered infectious disease model with the game inoculation process is established. First, the basic regeneration number R_0 of the model is obtained, and the positive and bounded connections of the system are proved. second, the stability of each equilibrium point is discussed by analyzing the characteristic equations of the system. Next, by taking ω as the parameter, the conditions for the occurrence of Hopf bifurcation are obtained. Furthermore, we use the method of parameter estimation to analyze the influence of each parameter on this system. Finally, through a numerical simulation, we verify all previous conclusions. Of course, symmetry provides a tractable framework for analyzing vaccination games but may overlook heterogeneity-driven phenomena.

Keywords: dynamic analysis; SIR epidemic model; game vaccination behavior
Mathematics Subject Classification: 37N25

1. Introduction

Infectious diseases have been a persistent threat to human health and societal stability throughout history. Epidemic outbreaks not only generate substantial morbidity and mortality, but also impose profound disruptions on economic and social systems. To counter these challenges, a diverse arsenal of control strategies has been devised, among which vaccination is widely regarded as one of the most efficacious public health interventions [1–4].

However, the decision to vaccinate transcends purely biomedical considerations; it is profoundly shaped by individual cognition, social behavior, and economic incentives. The bidirectional coupling between an epidemic's dynamics and human decision-making has therefore prompted researchers to invoke game-theoretic frameworks in vaccination studies, with the aim of elucidating how individual

strategic choices modulate disease transmission [5–7]. In our setting, the "game" consists of parents deciding whether to vaccinate newborns. The players are the parents, the strategies are "vaccinate" or "not vaccinate", and their payoffs depend on the perceived infection risk and the perceived vaccine risk, evolving over time via imitation.

Existing studies have made substantial advances in elucidating the dynamics of vaccination and disease transmission. For instance, Chhabra [8] highlighted manufacturing issues and the effects of vaccines by analyzing surveys conducted in India, where the respondents were asked about their views and concerns regarding the national vaccination programme. They carried out a mathematical analysis of adverse events following immunization (AEFI) and vaccine adverse events reporting system (VAERS). For a non-zero proportion of vaccinated individuals, their model predicts a new state in which the disease spreads but eventually becomes extinct. A new state occurs when the proportion of vaccinated individuals exceeds a certain critical value; this critical value increases with the infection rate, up to an asymptotic value strictly less than unity. Beyond this value, disease extinction occurs regardless of the infection rate.

Nunuvero [9] explored the effects of adherence to vaccination and health protocols on an epidemic's dynamics using an extended susceptible–infectious–recovered model framework. Their model incorporated critical factors such as birth and death rates, infection and recovery rates, vaccination uptake, and limited immunity. By analyzing various scenarios, the study revealed two key findings. First, strict adherence to health protocols can significantly reduce disease transmission and, as a result, lessen the dependency on mass vaccination program; second, robust vaccination strategies can compensate for lower adherence to health protocols.

Deka and Bhattacharyya [10] investigated the public health implications of pathogen competition under social interaction and individual choice. Their results suggest that appropriate risk communication about disease severity is crucial for reducing the chances of strains' invasion. Consequently, understanding pathogen competition in the presence of social behaviour and strategic choice can be an important component of decision-makers' strategies.

Joe and Bauch [11] showed that adaptive social behaviour can allow mutant strains to invade in realistic epidemiological scenarios, even if the basic reproduction number of the mutant strain is lower than that of the resident strain. Surprisingly, in some cases, increasing the perceived severity of resident strains may actually promote the invasion of more deadly mutant strains. These insights suggest that for some applications, adaptive social behaviors must be incorporated into models of viral pathogens' emergence in order to better inform public health control strategies.

Beyond these contributions, there has also been important work on epidemic models with waning immunity and information-dependent vaccination. For example, Saade et al. [12] proposed delay epidemic models that explicitly a incorporate loss of immunity over time, while Buonomo et al. [13] analyzed the global stability of an SIR model in which the vaccination rate depends on information about the disease's spread. In contrast to these studies, which typically focus either on waning immunity or on information-driven vaccination, the present work simultaneously combines waning immunity with imitation-based vaccination behaviour and nonlinear (saturated) incidence, thereby bridging these two lines of research within a unified framework.

In parallel, several works have analyzed behavioural vaccination in game-theoretic or information-dependent frameworks, including Buonomo et al. [13], while Xiao and Ruan [23] studied an SIR model with nonmonotone (saturated) incidence. Compared with these contributions, our model differs in three

main aspects:

(i) A the incidence level, we combine saturated transmission with an explicit behavioural feedback;

(ii) we incorporate waning immunity and imitation dynamics simultaneously, rather than treating them in separate models;

(iii) Imitation dynamics are coupled to the epidemiological variables through decisions regarding vaccination of newborns, so that parental strategies directly determine whether newborns enter the susceptible or recovered class.

Recent years have also witnessed a rapidly growing body of work on information and awareness diffusion and their impact on epidemic thresholds. These studies show that the spread of risk awareness, media-driven information, and behaviourally adaptive responses can substantially modify classical SIR-type predictions by altering effective contact rates and generating new threshold phenomena. For example, some models explicitly couple awareness propagation with disease transmission on multiplex or temporal networks, demonstrating that awareness-induced behavioural changes may delay, suppress, or reshape epidemic outbreaks [14–18]. Such awareness-based frameworks enrich the traditional epidemic modelling paradigm and provide a complementary perspective to imitation-based vaccination behaviour.

These findings collectively underscore the critical role of behavioral compliance and vaccination programs in shaping the trajectory of epidemics. Regarding the use of symmetry assumptions in SIR-type models, it is important to examine how symmetry simplifies the mathematical structure and how this assumption influences the resulting vaccination strategies. In our vaccination game framework, symmetry refers to a homogeneous behavior assumption among parents: All individuals face the same perceived vaccination cost and infection risk and update their decisions according to the same imitation rule.

Mathematically, this symmetry allows us to describe the behavioural state of the whole population by a single scalar variable $x(t)$ (the fraction of vaccinating parents), instead of tracking multiple subgroups $x_1(t), x_2(t), \ldots$ with different payoff structures. This reduction from a high-dimensional system to a four-dimensional one makes it possible to derive explicit formulas for the equilibria and to obtain analytic Hopf bifurcation conditions. From the viewpoint of vaccination strategies, the symmetry assumption means that the model predicts a uniform population-level vaccination coverage, i.e, the same imitation rule and equilibrium strategy apply to all parents.

In heterogeneous populations (e.g. heterogeneity in age, risk, socioeconomic status, or access to vaccination), one would expect different groups to adopt different vaccination levels. Such heterogeneity-driven effects are not captured by the present model and are explicitly discussed as a limitation and a direction for future work. We emphasize that the symmetry applies to the behavioral imitation part rather than to the epidemiological compartments.

In addition, we explicitly relate this assumption to the standard homogeneous population framework of evolutionary game theory, in which a symmetric payoff structure and identical update rules permit the behavioral state to be represented by a single frequency variable $x(t)$; see, for example, Bauch [19] and the general framework in Hofbauer and Sigmund [20]. Building on this foundation, our work extends the SIR modelling framework to incorporate game-theoretic approaches to vaccination behavior. By analyzing how individuals' decision-making under varying levels of risk perception and social influence impacts vaccination uptake, this study aims to offer deeper insights into optimizing epidemic control strategies.

1.1. Behavioral imitation dynamics

To better capture the adaptive nature of vaccination decisions, we integrate a game-theoretic imitation dynamic into the classical SIR framework. In this context, parents are treated as strategic decision-makers who weigh the perceived risks of vaccination against the perceived risks of infection, and individuals may revise their strategy by imitating those who are perceived to achieve higher payoffs. Following the formulation of Bauch [19] and the general evolutionary game framework in Hofbauer and Sigmund [20], we adopt a vaccination function that describes imitation-based behavioural dynamics.

Specifically, the evolution of the proportion $x(t)$ of vaccinators is governed by the imitation equation

$$\frac{\mathrm{d}x}{\mathrm{d}t} = kx(1-x)(-r_v + r_i m I),$$

where k denotes the sampling–imitation rate, i.e, the rate at which individuals sample others and imitate their strategies. The parameter r_v is the perceived vaccine risk, r_i is the perceived infection risk, and m measures sensitivity to prevalence, quantifying how sensitively individuals adjust their vaccinating behaviour in response to changes in the disease prevalence $I(t)$.

More precisely, we write

$$-r_v + r_i m I \;=\; r_v\Big(-1 + \frac{r_i m}{r_v} I\Big) \quad \text{and define} \quad \omega := \frac{r_i m}{r_v},$$

absorbing the prefactor r_v into the imitation rate k (or into a rescaling of time). Following Bauch [19] and subsequent work on imitation dynamics, we normalize the perceived disutility of vaccination to 1, while the infection-related perceived loss is taken to be proportional to the prevalence $I(t)$ and scaled by the sensitivity parameter ω. Thus, by absorbing the product $r_i m$ into a single parameter ω, the payoff difference between vaccinating and not vaccinating can be written as

$$U_{\text{vaccinate}} - U_{\text{non-vaccinate}} = -1 + \omega I.$$

In particular, when $\omega I < 1$, the perceived vaccination cost dominates and non-vaccination is favoured, whereas when $\omega I > 1$, the perceived infection risk dominates and vaccination becomes individually beneficial. This leads to the rescaled imitation equation

$$\frac{\mathrm{d}x}{\mathrm{d}t} = kx(1-x)(-1 + \omega I),$$

which is the behavioural component coupled to the SIR epidemic dynamics in our model.

The prevalence $I(t)$ is determined by a compartmental SIR epidemic model with births and deaths [21, 22]. Compartmental models divide the population into mutually exclusive categories according to their epidemiological status and define ordinary differential equations that govern the flow between compartments. Here, we make the standard assumption that the rate at which newly infected individuals arise is proportional to the product of the densities of susceptible and infected individuals.

The advantage of using game theory in this epidemiological setting lies in its ability to incorporate human behavioral responses into disease dynamics. While traditional models typically treat vaccination as a fixed-rate intervention, game-theoretic models allow vaccination uptake to evolve

adaptively according to individuals' risk perception and social influence. This behavioural–epidemiological coupling can reveal threshold effects, oscillatory dynamics, and bifurcation phenomena that purely biological models cannot capture, thereby providing more realistic insights into optimal epidemic control strategies.

The vaccination game with imitation dynamics is described by the system of ordinary differential equations (ODEs)

$$\begin{cases} \dfrac{\mathrm{d}S}{\mathrm{d}t} = \Lambda - \mu x - \mu S - \beta S I, \\ \dfrac{\mathrm{d}I}{\mathrm{d}t} = \beta S I - \mu I - \gamma I, \\ \dfrac{\mathrm{d}R}{\mathrm{d}t} = \gamma I + \mu x - \mu R, \\ \dfrac{\mathrm{d}x}{\mathrm{d}t} = kx(1-x)(-1+\omega I). \end{cases} \tag{1.1}$$

While these studies have advanced the field, they often rely on simplifying assumptions that do not fully capture the complexities of real-world epidemics and human behaviour. Specifically, many models assume bilinear incidence rates and lifelong immunity, which are not applicable to diseases with waning immunity or transmission saturation effects. Moreover, the interaction between social imitation in vaccination decisions, and these realistic epidemiological features remains underexplored.

Building upon previous analyses and motivated by the considerations above, we incorporate the nonmonotone (saturated) incidence rate proposed by Xiao and Ruan [23] to obtain a more realistic transmission function. Accordingly, we propose the following modified model:

$$\begin{cases} \dfrac{\mathrm{d}S}{\mathrm{d}t} = \Lambda - \mu x - \mu S + \delta R - \dfrac{\beta S I}{1+\alpha I}, \\ \dfrac{\mathrm{d}I}{\mathrm{d}t} = \dfrac{\beta S I}{1+\alpha I} - \mu I - \gamma I, \\ \dfrac{\mathrm{d}R}{\mathrm{d}t} = \gamma I + \mu x - \mu R - \delta R, \\ \dfrac{\mathrm{d}x}{\mathrm{d}t} = kx(1-x)(-1+\omega I), \end{cases} \tag{1.2}$$

with the initial conditions $S(0) > 0$, $I(0) > 0$, $R(0) > 0$, and $x(0) > 0$.

In the nonlinear incidence term $\dfrac{\beta S I}{1+\alpha I}$, the parameter $\alpha > 0$ measures the *saturation strength* of transmission when the number of infectious individuals I becomes large. Biologically, this means that the effective contact rate does not grow indefinitely with I but is reduced by contact saturation, limited medical or public health resources, and behavioral avoidance (e.g, individuals voluntarily reducing contacts or keeping distance from infectious cases). Following Xiao and Ruan [23], this saturated form provides a bounded and more realistic infection rate in the high-prevalence regime, in contrast to the standard bilinear incidence $\beta S I$, which may overestimate transmission when I is large.

The formulation of Systems (1.1) and (1.2) is based on the following biological and epidemiological assumptions:

- The total population is divided into four mutually exclusive classes: Susceptible individuals $S(t)$, infectious individuals $I(t)$, recovered individuals with temporary immunity $R(t)$, and the proportion of vaccinators $x(t)$.

- Births occur at a constant rate Λ, and natural deaths occur at a rate μ in all epidemiological classes.
- Recovered individuals lose immunity at a rate δ and return to the susceptible class, representing waning immunity.
- Disease transmission follows the saturated (nonmonotone) incidence rate $\dfrac{\beta S I}{1+\alpha I}$ discussed above, which accounts for contact saturation, behavioral changes, and resource constraints when the number of infectious individuals is large.
- Vaccination is modelled as a game-theoretic imitation process: Parents decide whether to vaccinate newborns according on the perceived payoffs, leading to the imitation dynamics $\dfrac{\mathrm{d}x}{\mathrm{d}t} = kx(1-x)(-1+\omega I)$.
- Vaccination affects the flow of newborns: A proportion $x(t)$ of newborns are vaccinated immediately upon birth, contributing directly to the recovered class R, while the remaining proportion $(1-x(t))$ enters the susceptible class S.

For convenience, we summarize the biological interpretation and units of the main parameters used in the model in Table 1.

Table 1. Biological interpretation and units of the parameters used in the model. Time is measured in days, and S, I, R denote fractions of the population.

Parameter	Description	Units	Typical range
Λ	Recruitment/birth rate	day^{-1}	10^{-3}–10^{-1}
μ	Natural death rate	day^{-1}	10^{-3}–10^{-1}
β	Transmission rate	day^{-1}	10^{-2}–1
γ	Recovery rate from infection	day^{-1}	10^{-2}–1
δ	Waning immunity rate ($R \to S$)	day^{-1}	10^{-4}–10^{-2}
α	Saturation parameter in incidence	dimensionless	10^{-4}–10^{-1}
k	Sampling–imitation rate	day^{-1}	10^{-4}–10^{-2}
ω	Sensitivity to prevalence	dimensionless	10^{0}–10^{3}

Compared with the classical framework in [23], our model incorporates three key modifications:

- We extend the SIR model of [23], which assumes permanent immunity, by introducing a waning immunity mechanism ($R \to S$ at rate δ).
- We integrate game theoretic imitation dynamics into the vaccination decision process via the variable $x(t)$, which is absent in [23].
- We allow the vaccination decision $x(t)$ to dynamically interact with the epidemiological variables through the recruitment terms $\Lambda - \mu x$ and μx in the S and R equations, respectively, thereby coupling behavioral and epidemiological dynamics.

These modifications enable the joint analysis of an epidemic's progression and adaptive vaccination behaviour, revealing bifurcation and oscillatory dynamics that cannot arise in the model of [23].

A standard next-generation matrix calculation (see Section 2) shows that the basic reproduction

number of System (1.2) is

$$R_0 = \frac{\beta S^0}{\mu + \gamma} = \frac{\beta}{\mu + \gamma} \frac{\Lambda}{\mu},$$

where $S^0 = \Lambda/\mu$ is the susceptible level at the disease-free equilibrium. Since at this equilibrium the nonlinear incidence term

$$\frac{\beta S I}{1 + \alpha I}$$

degenerates to the bilinear form $\beta S I$ (because $I = 0$), the expression of R_0 coincides with that of the classical SIR model and does not explicitly depend on the waning immunity rate δ or on the saturation parameter α. These parameters influence the long-term dynamics (such as the existence and stability of endemic equilibria and possible oscillations), but they do not modify the initial invasion threshold encoded in R_0.

The inclusion of these features is motivated by several gaps in the current literature. Traditional SIR models often oversimplify transmission dynamics and immunity mechanisms, potentially leading to inaccurate predictions of the disease's spread and control measures. By incorporating a nonmonotone incidence rate and waning immunity, our model better mirrors the complexities of real-world epidemics.

Vaccination is not only a public health intervention but also a social behaviour influenced by individual and collective decision-making. While previous studies have applied game theory to vaccination, few have simultaneously considered social imitation and realistic epidemiological dynamics. Our model addresses this by embedding imitation dynamics within a more nuanced epidemiological framework.

Understanding the combined influence of behavioural and epidemiological factors is crucial for designing effective vaccination campaigns and disease control policies. Our analysis aims to uncover critical thresholds and nonlinear phenomena that can guide the optimization of intervention strategies.

1.2. Main contributions and organization of the paper

The main contributions of this work are summarized as follows.

(1) We develop a novel epidemic–game theoretic framework that incorporates a nonmonotone incidence rate, waning immunity, and vaccination behavior driven by social imitation. In particular, newborns are dynamically allocated between the susceptible and recovered classes according to the behavioral variable $x(t)$, thus creating a birth–vaccination coupling between parental strategies and epidemiological compartments. This formulation enables a more realistic description of the transmission dynamics and behavioral responses in the context of vaccination.
(2) We conduct a comprehensive qualitative analysis of the proposed model. This includes proving the positivity and boundedness of solutions, identifying all possible equilibria, and establishing their local and global stability. In particular, Lyapunov functions are explicitly constructed to demonstrate the global asymptotic stability of certain equilibria, and Hopf bifurcation conditions at the interior equilibrium are derived, revealing the potential for sustained oscillatory behaviour in both the infection's prevalence and vaccination uptake.
(3) We perform numerical simulations and a global sensitivity analysis (via Latin hypercube sampling and partial rank correlation coefficients) to assess the influence of key epidemiological

and behavioural parameters. The numerical results confirm the theoretical predictions and illustrate how parameter variations can modulate the amplitude and persistence of epidemic outbreaks, thereby providing qualitative insights for optimizing disease control strategies.

The remainder of the paper is organized as follows. In Section 2, we discuss the positivity of solutions and establish a uniformly bounded invariant region for System (1.2). In Section 3, we derive all equilibria of the system and analyse the local stability of each equilibrium; Lyapunov functions are constructed for the boundary equilibria E_3 and E_4, and their global stability is proven. In Section 4, we analyze the local stability of the interior equilibrium E_5 and show that the system can undergo a Hopf bifurcation at this point. In Section 5, we present numerical simulations and the global sensitivity analysis to illustrate and support the theoretical results. Finally, in Section 6, we summarize our main findings and outline several directions for future research.

2. Basic properties of the model

Equilibria of System (1.2)

Equilibria are points (S^*, I^*, R^*, x^*) at which the right-hand sides of (1.2) vanish. Thus we require

$$0 = \Lambda - \mu x^* - \mu S^* + \delta R^* - \frac{\beta S^* I^*}{1 + \alpha I^*}, \tag{2.1}$$

$$0 = \frac{\beta S^* I^*}{1 + \alpha I^*} - (\mu + \gamma) I^*, \tag{2.2}$$

$$0 = \gamma I^* + \mu x^* - (\mu + \delta) R^*, \tag{2.3}$$

$$0 = k x^* (1 - x^*)(-1 + \omega I^*). \tag{2.4}$$

Equation (2.4) implies that at an equilibrium, one of the following holds:

$$x^* = 0, \qquad x^* = 1, \qquad \text{or} \qquad I^* = \frac{1}{\omega}.$$

We treat these three cases separately.

Disease-free equilibria (DFE), $I^* = 0$.

Set $I^* = 0$ in (2.2) and (2.3). From (2.3), we obtain

$$R^* = \frac{\mu x^*}{\mu + \delta}.$$

Substituting $I^* = 0$ and this R^* into (2.1) yields

$$0 = \Lambda - \mu x^* - \mu S^* + \delta \frac{\mu x^*}{\mu + \delta},$$

hence

$$S^* = \frac{\Lambda}{\mu} - \frac{\mu}{\mu + \delta} x^*.$$

Because (2.4) with $I^* = 0$ allows $x^* = 0$ or $x^* = 1$, we obtain two disease-free equilibria

$$E_{DF,0} = \left(\tfrac{\Lambda}{\mu},\ 0,\ 0,\ 0\right), \tag{2.5}$$

$$E_{DF,1} = \left(\tfrac{\Lambda}{\mu} - \tfrac{\mu}{\mu+\delta},\ 0,\ \tfrac{\mu}{\mu+\delta},\ 1\right), \tag{2.6}$$

provided that the components are non-negative (in particular, one needs $\frac{\Lambda}{\mu} \geq \frac{\mu}{\mu+\delta}$ for $E_{DF,1}$ to have $S^* \geq 0$). Note that $S^* + R^* = \Lambda/\mu$ at both DFEs.

Endemic candidates with $I^* > 0$ and $x^* = 0$ or $x^* = 1$.

Assume $I^* > 0$. From (2.2), we obtain

$$\frac{\beta S^*}{1+\alpha I^*} = \mu + \gamma \quad \Longrightarrow \quad S^* = \frac{\mu+\gamma}{\beta}(1+\alpha I^*).$$

From (2.3), we have

$$R^* = \frac{\gamma I^* + \mu x^*}{\mu+\delta}.$$

Substitute S^* and R^* into (2.1). After rearrangement, one obtains a linear expression for I^* (for a fixed x^*):

$$I^* = \frac{\Lambda\beta(\delta+\mu) - \beta\mu^2 x^* - \mu(\delta\gamma + \delta\mu + \gamma\mu + \mu^2)}{\mu\Big(\alpha(\delta\gamma + \delta\mu + \gamma\mu + \mu^2) + \beta(\delta+\gamma+\mu)\Big)}. \tag{2.7}$$

Hence, for the two cases $x^* = 0$ and $x^* = 1$, we get two possible endemic equilibria (call them $E_*^{(0)}$ and $E_*^{(1)}$) with

$$S^* = \frac{\mu+\gamma}{\beta}(1+\alpha I^*), \qquad R^* = \frac{\gamma I^* + \mu x^*}{\mu+\delta},$$

and I^* is given by $(*)$ with $x^* = 0$ or $x^* = 1$. These equilibria exist (and are biologically admissible) only if the right hand side of $(*)$ is positive and produces $S^* > 0, R^* \geq 0$.

To link these existence conditions with the threshold quantity of the model, we recall that the basic reproduction number is computed via the next generation matrix at the DEF

$$E_{DF,0} = \left(\tfrac{\Lambda}{\mu}, 0, 0, 0\right).$$

At this point we have $I^* = 0$, so the nonlinear incidence term

$$\frac{\beta S I}{1+\alpha I}$$

reduces to the bilinear form $\beta S I$. Consequently, the basic reproduction number is

$$R_0 = \frac{\beta S^0}{\mu+\gamma} = \frac{\beta}{\mu+\gamma}\,\frac{\Lambda}{\mu},$$

where $S^0 = \Lambda/\mu$ is the level at of susceptibility $E_{DF,0}$. In particular, the waning immunity rate δ does not enter the next generation matrix and therefore does not affect R_0. If we normalize the total population so that $S^0 = \Lambda/\mu = 1$ (i.e, we work with proportions), this reduces to the classical form

$$R_0 = \frac{\beta}{\mu+\gamma},$$

and the condition $R_0 > 1$ is typically necessary for the existence of an endemic solution with $x^* = 0$.

Interior endemic with $I^* = \dfrac{1}{\omega}$ and $x^* \in (0, 1)$.

If $I^* = 1/\omega$, then (2.4) permits any $x^* \in [0, 1]$. To find an admissible x^*, one substitutes $I^* = 1/\omega$ into (2.2) and (2.1). From (2.2), we obtain

$$S^* = \frac{\mu + \gamma}{\beta}\Big(1 + \frac{\alpha}{\omega}\Big).$$

From (2.3), we have

$$R^* = \frac{\gamma/\omega + \mu x^*}{\mu + \delta}.$$

Substituting into (2.1) yields a linear equation for x^*; solving this equation gives

$$x^* = \frac{\Lambda\beta(\delta + \mu)\omega - \mu\omega(\delta\gamma + \mu(\delta + \gamma + \mu)) - \alpha(\delta\gamma\mu + \delta\mu^2 + \gamma\mu^2 + \mu^3)}{\beta\mu^2\omega}.$$

An interior endemic equilibrium with $I^* = 1/\omega$ exists if and only if the computed x^* lies in $(0, 1)$ and the corresponding S^*, R^* are non-negative.

According to the equilibrium computations above, we classify all equilibria according to whether all components are strictly positive (*positive equilibria*) or whether at least one component lies on the boundary (*boundary equilibria*):

- The DFEs

$$E_{DF,0} = \Big(\tfrac{\Lambda}{\mu},\, 0,\, 0,\, 0\Big),$$
$$E_{DF,1} = \Big(\tfrac{\Lambda}{\mu} - \tfrac{\mu}{\mu+\delta},\, 0,\, \tfrac{\mu}{\mu+\delta},\, 1\Big),$$

  are *boundary equilibria*, since the infectious class satisfies $I^* = 0$.
- The endemic equilibria $E^*(0)$ (with $x^* = 0$) and $E^*(1)$ (with $x^* = 1$) have $I^* > 0$ but the vaccination variable x lies on the boundary ($x = 0$ or $x = 1$), hence these are also *boundary equilibria*.
- The interior endemic equilibrium (with $I^* = 1/\omega$ and $x^* \in (0, 1)$) satisfies

$$S^* > 0, \qquad I^* > 0, \qquad R^* > 0, \qquad x^* > 0,$$

  i.e., all components are strictly positive, and is therefore the unique *positive equilibrium* of the system.

In summary, the model admits a single positive equilibrium arising from the coupling of behavioral dynamics with epidemiological transmission, whereas all other equilibria lie on the boundary of the feasible region.

In natural ecology, positiveness means that the population can survive, and boundedness means that the resources of the population are limited. Therefore, we will discuss the positiveness and boundedness of System (1.2).

Theorem 2.1. *All solutions of System* (1.2) *with non-negative initial data remain in $\mathbb{R}^4_+$ for all $t \geq 0$. Moreover, if*

$$S(0) > 0, \qquad I(0) > 0, \qquad R(0) > 0, \qquad x(0) > 0,$$

then $I(t)$, $R(t)$, and $x(t)$ stay strictly positive for all $t > 0$.

Proof. We show that each component of the solution of the model (1.2) cannot become negative, and that strictly positive initial data for I, R, and x remain strictly positive for all $t > 0$.

Positivity of $I(t)$. The equation for I can be written as

$$\frac{\mathrm{d}I}{\mathrm{d}t} = I\Big(\frac{\beta S}{1+\alpha I} - (\mu+\gamma)\Big).$$

When $I = 0$, the right-hand side vanishes. Hence, the hyperplane $I = 0$ is invariant and, by the uniqueness of the solutions, we have $I(t) \geq 0$ for all $t \geq 0$ whenever $I(0) \geq 0$. Moreover, since

$$\frac{\beta S}{1+\alpha I} - (\mu+\gamma) \;\geq\; -(\mu+\gamma),$$

we obtain

$$\frac{dI}{dt} \geq -(\mu+\gamma)\, I.$$

By Grönwall's inequality it follows that

$$I(t) \geq I(0)\, e^{-(\mu+\gamma)t},$$

so if $I(0) > 0$ then $I(t) > 0$ for all $t > 0$.

Positivity of $x(t)$. The behavioural variable satisfies

$$\frac{\mathrm{d}x}{\mathrm{d}t} = kx(1-x)(-1+\omega I).$$

Clearly, $x = 0$ implies $\dot{x} = 0$, so the hyperplane $x = 0$ is invariant and $x(t) \geq 0$ for all $t \geq 0$ whenever $x(0) \geq 0$. To see that $x(t)$ cannot reach 0 in finite time if $x(0) > 0$, we argue by contradiction: Assume that there is a $t_0 > 0$ such that $x(t_0) = 0$ and $x(t) > 0$ for all $t \in [0, t_0)$. By continuity, the solution $(S(t), I(t), R(t), x(t))$ is well-defined on a neighborhood of t_0, and the initial value problem for x with the data $x(t_0) = 0$ has the trivial solution $x \equiv 0$. By uniqueness of solutions to System (1.2), this would imply $x(t) \equiv 0$ on $[0, t_0]$, contradicting $x(0) > 0$. Hence $x(t) > 0$ for all $t > 0$.

Positivity of $R(t)$. For R, we have

$$\frac{\mathrm{d}R}{\mathrm{d}t} = \gamma I + \mu x - (\mu+\delta)R.$$

If $R = 0$ with $I, x \geq 0$, then $\dot{R} = \gamma I + \mu x \geq 0$, so the boundary $R = 0$ cannot be crossed to negative values. Moreover

$$\frac{\mathrm{d}R}{\mathrm{d}t} \geq -(\mu+\delta)\, R,$$

since $\gamma I + \mu x \geq 0$. By Grönwall's inequality

$$R(t) \geq R(0) e^{-(\mu+\delta)t},$$

so $R(t) \geq 0$ for all $t \geq 0$ and, in particular, $R(t) > 0$ for all $t > 0$ if $R(0) > 0$.

Positivity of $S(t)$. Consider the total population

$$N(t) = S(t) + I(t) + R(t).$$

Summing the first three equations of (1.2) gives

$$\frac{\mathrm{d}N}{\mathrm{d}t} = \Lambda - \mu N,$$

with the explicit solution

$$N(t) = \frac{\Lambda}{\mu} + (N(0) - \tfrac{\Lambda}{\mu})e^{-\mu t},$$

which is non-negative (and in fact is strictly positive for $t > 0$ if $N(0) > 0$). Since we have already shown that $I(t) \geq 0$ and $R(t) \geq 0$, it follows that

$$S(t) = N(t) - I(t) - R(t) \geq 0 \qquad \text{for all } t \geq 0.$$

Therefore, $S(t)$ cannot become negative.

Combining the arguments above, we conclude that any solution with non-negative initial data remains in $\mathbb{R}^4_+$ for all $t \geq 0$, and that $I(t)$, $R(t)$ and $x(t)$ remain strictly positive for all $t > 0$ whenever $I(0)$, $R(0)$, and $x(0)$ are strictly positive. This proves the theorem. □

Theorem 2.2 (Boundedness and positive invariance)**.** *For System* (1.2)*, if the initial data satisfy*

$$S(0) \geq 0, \quad I(0) \geq 0, \quad R(0) \geq 0, \quad x(0) \in [0, 1],$$

then the corresponding solution remains non-negative for all $t \geq 0$. Moreover, the total population

$$N(t) := S(t) + I(t) + R(t)$$

satisfies the scalar linear equation

$$\frac{\mathrm{d}N}{\mathrm{d}t} = \Lambda - \mu N,$$

whose solution is uniformly bounded and converges to Λ/μ as $t \to \infty$. In particular, $M > 0$ exists such that $0 \leq N(t) \leq M$ for all $t \geq 0$, and the set

$$\Omega := \{(S, I, R, x) \in \mathbb{R}^4 : \ S \geq 0, \ I \geq 0, \ R \geq 0, \ 0 \leq x \leq 1, \ 0 \leq N \leq \Lambda/\mu\}$$

is a positively invariant bounded region for System (1.2)*.*

Proof. Summing the first three equations of System (1.2) gives

$$\begin{aligned}\frac{\mathrm{d}N}{\mathrm{d}t} &= (\Lambda - \mu x - \mu S + \delta R - \tfrac{\beta S I}{1+\alpha I}) + (\tfrac{\beta S I}{1+\alpha I} - (\mu + \gamma)I) + (\gamma I + \mu x - (\mu + \delta)R) \\ &= \Lambda - \mu(S + I + R) = \Lambda - \mu N,\end{aligned}$$

a linear ODE with explicit solution

$$N(t) = \frac{\Lambda}{\mu} + (N(0) - \tfrac{\Lambda}{\mu})e^{-\mu t},$$

which shows that $\limsup_{t\to\infty} N(t) \leq \Lambda/\mu$.

Next, for x we note

$$\dot{x} = kx(1-x)(-1+\omega I).$$

At the boundary $x = 0$ or $x = 1$, the derivative vanishes, so by uniqueness, the flow cannot cross these boundaries. Thus if $x(0) \in [0,1]$, then $x(t) \in [0,1]$ for all $t \geq 0$.

Finally, Theorem 2.1 already guarantees that S, I, R remain non-negative for no-nnegative initial data (and strictly positive if strictly positive initially). Combining these facts shows that

$$\Omega = \{(S,I,R,x) : S \geq 0,\ I \geq 0,\ R \geq 0,\ 0 \leq x \leq 1,\ 0 \leq N \leq \Lambda/\mu\}$$

is positively invariant and bounded. □

3. Exisetence and local stability of equilibria

In this section, we will discuss the existence and local stability of System (1.2). By some calculation, System (1.2) have five equilibria as follows.

Theorem 3.1. *(Local stability of DEFs* (1.2) *and the DEFs*

$$E_{DF,0} = \left(\tfrac{\Lambda}{\mu}, 0, 0, 0\right), \qquad E_{DF,1} = \left(\tfrac{\Lambda}{\mu} - \tfrac{\mu}{\mu+\delta}, 0, \tfrac{\mu}{\mu+\delta}, 1\right),$$

(the latter exists whenever $\frac{\Lambda}{\mu} \geq \frac{\mu}{\mu+\delta}$ *so that* $S^* \geq 0$*). Let* $R_0 = \dfrac{\beta}{\mu+\gamma}$*. Then*

(1) $E_{DF,0}$ *is locally asymptotically stable if* $R_0 < 1$ *and unstable if* $R_0 > 1$*;*
(2) $E_{DF,1}$ *is unstable (in particular, the vaccination direction* x *is unstable when* $I^* = 0$*).*

Proof. Compute the Jacobian J of System (1.2). Evaluating the derivatives at

$$E_{DF,0} = (S^0, I^0, R^0, x^0) = (\Lambda/\mu, 0, 0, 0)$$

yields

$$J(E_{DF,0}) = \begin{pmatrix} -\mu & -\beta\frac{\Lambda}{\mu} & \delta & -\mu \\ 0 & \beta\frac{\Lambda}{\mu} - (\mu+\gamma) & 0 & 0 \\ 0 & \gamma & -(\mu+\delta) & \mu \\ 0 & 0 & 0 & -k \end{pmatrix}.$$

The Jacobian can be rearranged into a block upper triangular form, and its eigenvalues are given by the diagonal elements of each block. Its eigenvalues are the diagonal entries

$$\lambda_1 = -\mu, \quad \lambda_2 = \beta\frac{\Lambda}{\mu} - (\mu+\gamma), \quad \lambda_3 = -(\mu+\delta), \quad \lambda_4 = -k.$$

Hence all eigenvalues have a negative real part if and only if $\beta\frac{\Lambda}{\mu} - (\mu+\gamma) < 0$, i.e.

$$\frac{\beta}{\mu+\gamma} \cdot \frac{\Lambda}{\mu} < 1.$$

Under the common normalization $\Lambda/\mu = 1$ (proportions), this condition is exactly $R_0 < 1$. Thus $E_{DF,0}$ is locally asymptotically stable when $R_0 < 1$ and unstable when $R_0 > 1$.

For $E_{DF,1}$ evaluate the Jacobian at $x^* = 1,\ I^* = 0,\ R^* = \mu/(\mu+\delta), and\ S^* = \Lambda/\mu - \mu/(\mu+\delta)$. The partial derivative of the right-hand side of the x–equation with respect to x is

$$\frac{\partial}{\partial x}(kx(1-x)(-1+\omega I))\Big|_{E_{DF,1}} = k(1-2x^*)(-1+\omega I^*)\Big|_{x^*=1,I^*=0} = k > 0,$$

so the linearization has a positive eigenvalue $+k$, and therefore, $E_{DF,1}$ is unstable (at least in the vaccination direction). This completes the proof. □

Theorem 3.2. *Let $E_3 = (S^*, I^*, R^*, x^* = 0)$ be an endemic equilibrium of system* (1.2)*, i.e., $I^* > 0$ and (S^*, I^*, R^*) satisfy the equilibrium relations. Let $J(E_3)$ denote the Jacobian of System* (1.2) *evaluated at E_3. Then the characteristic polynomial of $J(E_3)$ factors as*

$$\det(\lambda I - J(E_3)) = (\lambda - k(\omega I^* - 1))\, p_3^{(3)}(\lambda),$$

where

$$p_3^{(3)}(\lambda) = \lambda^3 + A_1\lambda^2 + A_2\lambda + A_3$$

is the characteristic polynomial of the $S-I-R$ block. In particular:

(1) A necessary condition for local asymptotic stability is $k(\omega I^* - 1) < 0$, i.e., $\omega I^* < 1$.
(2) If, in addition, the Routh–Hurwitz conditions

$$A_1 > 0, \qquad A_3 > 0, \qquad A_1A_2 > A_3$$

hold for the coefficients A_1, A_2, A_3 computed below, then all eigenvalues have a negative real part and E_3 is locally asymptotically stable.

Proof. The Jacobian of the $S-I-R$ subsystem at E_3 has the form

$$A = \begin{pmatrix} a_{11} & a_{12} & a_{13} \\ a_{21} & a_{22} & 0 \\ 0 & a_{32} & a_{33} \end{pmatrix},$$

with the explicit entries (evaluated at E_3)

$$\begin{aligned} a_{11} &= -\mu - \frac{\beta I^*}{1+\alpha I^*}, & a_{12} &= -\frac{\beta S^*}{(1+\alpha I^*)^2}, & a_{13} &= \delta, \\ a_{21} &= \frac{\beta I^*}{1+\alpha I^*}, & a_{22} &= \frac{\beta S^*}{(1+\alpha I^*)^2} - (\mu+\gamma), & a_{32} &= \gamma, \\ a_{33} &= -(\mu+\delta). \end{aligned}$$

From the standard determinant identities for a 3×3 matrix, the coefficients of $p_3^{(3)}(\lambda) = \lambda^3 + A_1\lambda^2 +$

$A_2\lambda + A_3$ are:

$$
\begin{aligned}
A_1 &= -(a_{11} + a_{22} + a_{33}) = 3\mu + \gamma + \delta + \frac{\beta I^*}{1+\alpha I^*} - \frac{\beta S^*}{(1+\alpha I^*)^2},\\
A_2 &= (a_{11}a_{22} - a_{12}a_{21}) + (a_{11}a_{33}) + (a_{22}a_{33})\\
&= \big(-\mu - \tfrac{\beta I^*}{1+\alpha I^*}\big)\big(\tfrac{\beta S^*}{(1+\alpha I^*)^2} - (\mu+\gamma)\big) + \tfrac{\beta S^*\beta I^*}{(1+\alpha I^*)^3}\\
&\quad + \big(-\mu - \tfrac{\beta I^*}{1+\alpha I^*}\big)\big(-(\mu+\delta)\big) + \big(\tfrac{\beta S^*}{(1+\alpha I^*)^2} - (\mu+\gamma)\big)\big(-(\mu+\delta)\big),\\
A_3 &= -\det(A) = -\big(a_{11}a_{22}a_{33} - a_{12}a_{21}a_{33} + a_{13}a_{21}a_{32}\big)\\
&= -\big(-\mu - \tfrac{\beta I^*}{1+\alpha I^*}\big)\big(\tfrac{\beta S^*}{(1+\alpha I^*)^2} - (\mu+\gamma)\big)\big(-(\mu+\delta)\big)\\
&\quad + \tfrac{\beta S^*\beta I^*}{(1+\alpha I^*)^3}(\mu+\delta) - \delta\,\tfrac{\beta I^*}{1+\alpha I^*}\,\gamma.
\end{aligned}
$$

Because the vaccination equation decouples at $x^* = 0$, its eigenvalue is $k(\omega I^* - 1)$. The Jacobian is block triangular, and hence the full characteristic polynomial is the product of the vaccination eigenvalue factor $(\lambda - k(\omega I^* - 1))$ and $p_3^{(3)}(\lambda)$. Applying the Routh–Hurwitz conditions for the cubic $p_3^{(3)}(\lambda)$ together with $k(\omega I^* - 1) < 0$ yields the desired local asymptotic stability criterion. □

Theorem 3.3 (Boundary equilibrium E_4 and local stability)**.** *Assume that the parameter set is such that System* (1.2) *admits the boundary equilibrium*

$$E_4 = (S^*, I^*, R^*, x^*) = (S^*, I^*, R^*, 1),$$

where

$$I^* = \frac{(\mu+\gamma)(\mu+\delta)\mu - (\mu-\delta)\beta}{\beta\delta\gamma - \mu\alpha(\mu+\delta) - \beta(\mu+\delta)(\mu+\gamma)}, \qquad S^* = \frac{\mu+\gamma}{\beta}(1+\alpha I_*), \qquad R^* = \frac{\gamma I_* + \mu}{\mu+\delta},$$

and $I_* > 0$, $S^* > 0$, $R^* > 0$. Let J^* be the Jacobian of system (1.2) *at E_4. Use*

$$p_3^{(4)}(\lambda) = \lambda^3 + B_1\lambda^2 + B_2\lambda + B_3$$

the characteristic polynomial of its 3×3 epidemiological block, and

$$c_{44} = k(1 - \omega I_*)$$

the eigenvalue corresponding to the vaccination direction. Then E_4 is locally asymptotically stable if and only if

$$c_{44} < 0 \quad (\textit{i.e. } \omega I_* > 1)$$

and the Routh–Hurwitz conditions for $p_3^{(4)}$ hold:

$$B_1 > 0, \qquad B_3 > 0, \qquad B_1B_2 > B_3.$$

In this case all eigenvalues of J^* have negative real parts.

Proof. Directly compute the partial derivatives of the right-hand sides of System (1.2) to obtain the Jacobian and evaluate it at E_4. The epidemiological 3×3 block A has the form

$$A = \begin{pmatrix} a_{11} & a_{12} & a_{13} \\ a_{21} & a_{22} & 0 \\ 0 & a_{32} & a_{33} \end{pmatrix},$$

where (with all quantities evaluated at E_4)

$$\begin{aligned} a_{11} &= -\mu - \frac{\beta I^*}{1+\alpha I^*}, \quad a_{12} = -\frac{\beta S^*}{(1+\alpha I^*)^2}, & a_{13} &= \delta, \\ a_{21} &= \frac{\beta I^*}{1+\alpha I^*}, & a_{22} &= \frac{\beta S^*}{(1+\alpha I^*)^2} - (\mu+\gamma), \quad a_{32} = \gamma, \\ a_{33} &= -(\mu+\delta). \end{aligned}$$

From the standard determinant identities for a 3×3 matrix, the coefficients of $p_3^{(4)}(\lambda) = \lambda^3 + B_1\lambda^2 + B_2\lambda + B_3$ are

$$\begin{aligned} B_1 &= -(a_{11}+a_{22}+a_{33}) = 3\mu + \gamma + \delta + \frac{\beta I^*}{1+\alpha I^*} - \frac{\beta S^*}{(1+\alpha I^*)^2}, \\ B_2 &= (a_{11}a_{22} - a_{12}a_{21}) + (a_{11}a_{33}) + (a_{22}a_{33}) \\ &= \big(-\mu - \tfrac{\beta I^*}{1+\alpha I^*}\big)\big(\tfrac{\beta S^*}{(1+\alpha I^*)^2} - (\mu+\gamma)\big) + \tfrac{\beta S^* \beta I^*}{(1+\alpha I^*)^3} \\ &\quad + \big(-\mu - \tfrac{\beta I^*}{1+\alpha I^*}\big)\big(-(\mu+\delta)\big) + \big(\tfrac{\beta S^*}{(1+\alpha I^*)^2} - (\mu+\gamma)\big)\big(-(\mu+\delta)\big), \\ B_3 &= -\det(A) = -(a_{11}a_{22}a_{33} - a_{12}a_{21}a_{33} + a_{13}a_{21}a_{32}) \\ &= -\big(-\mu - \tfrac{\beta I^*}{1+\alpha I^*}\big)\big(\tfrac{\beta S^*}{(1+\alpha I^*)^2} - (\mu+\gamma)\big)\big(-(\mu+\delta)\big) \\ &\quad + \tfrac{\beta S^* \beta I^*}{(1+\alpha I^*)^3}(\mu+\delta) - \delta\,\tfrac{\beta I^*}{1+\alpha I^*}\,\gamma. \end{aligned}$$

The vaccination direction derivative is

$$\partial_x(kx(1-x)(-1+\omega I))\big|_{E_4} = k(1-2x^*)(-1+\omega I^*) = k(1-\omega I^*) = c_{44}.$$

Because J^* is block upper triangular, its characteristic polynomial factors into the product of the linear factor $(\lambda - c_{44})$ and the cubic characteristic polynomial $p_3^{(4)}(\lambda)$ of A. By the Routh–Hurwitz criterion for a cubic, the three inequalities $B_1 > 0,\ B_3 > 0, and\ B_1B_2 > B_3$ are necessary and sufficient for all roots of $p_3^{(4)}$ to have negative real parts. Together with $c_{44} < 0$, this implies that all four eigenvalues of J^* have negative real parts. Hence, E_4 is locally asymptotically stable under the stated conditions. □

Lemma 3.1 (Routh–Hurwitz data for the S–I–R block)**.** *Let $E^* = (S^*, I^*, R^*, x^*)$ be the interior equilibrium of System* (1.2) *given in Lemma 4.1. Consider the following Jacobian of the S–I–R subsystem evaluated at E^**

$$A = \begin{pmatrix} a_{11} & a_{12} & a_{13} \\ a_{21} & a_{22} & 0 \\ 0 & a_{32} & a_{33} \end{pmatrix},$$

where, with $D := 1 + \alpha I^*$

$$a_{11} = -\mu - \frac{\beta I^*}{D}, \quad a_{12} = -\frac{\beta S^*}{D^2}, \qquad a_{13} = \delta,$$
$$a_{21} = \frac{\beta I^*}{D}, \qquad a_{22} = \frac{\beta S^*}{D^2} - (\mu + \gamma), \quad a_{32} = \gamma,$$
$$a_{33} = -(\mu + \delta).$$

The characteristic polynomial of A is

$$p_3^{(*)}(\lambda) = \lambda^3 + C_1\lambda^2 + C_2\lambda + C_3,$$

with coefficients

$$C_1 = -(a_{11} + a_{22} + a_{33}),$$
$$C_2 = a_{11}a_{22} - a_{12}a_{21} + a_{11}a_{33} + a_{22}a_{33},$$
$$C_3 = a_{33}(a_{11}a_{22} - a_{12}a_{21}) + a_{13}a_{21}a_{32}.$$

Moreover, for the admissible parameter region considered in this paper, these coefficients satisfy

$$C_1 > 0, \qquad C_3 > 0, \qquad C_1C_2 > C_3.$$

In particular, the Routh–Hurwitz conditions for $p_3^{(*)}$ *hold, and all eigenvalues of the S–I–R linearization at* E^* *have negative real parts.*

Theorem 3.4 (Local stability of the interior equilibrium)**.** *Let* $E^* = (S^*, I^*, R^*, x^*)$ *be an admissible interior equilibrium of System* (1.2) *with*

$$I^* = \frac{1}{\omega}, \qquad 0 < x^* < 1, \qquad S^* > 0, \quad R^* > 0.$$

Let A be the Jacobian matrix of the S–I–R subsystem evaluated at E^* *and let*

$$p_3^{(*)}(\lambda) = \lambda^3 + C_1\lambda^2 + C_2\lambda + C_3$$

be its characteristic polynomial as in Lemma 3.1. For the admissible parameter region considered in this paper, Lemma 3.1 ensures that

$$C_1 > 0, \qquad C_3 > 0, \qquad C_1C_2 > C_3,$$

so all eigenvalues of the S–I–R linearization have negative real parts. Then E^* *is locally asymptotically stable: there is a neighborhood U of* E^* *such that any solution of* (1.2) *with the initial condition in U converges to* E^* *as* $t \to \infty$.

Proof. We first outline the strategy of the proof. We construct a Lyapunov function that combines a Volterra-type term for the epidemiological variables (S, I, R) with a quadratic term in the behavioural variable x. We then show that under the Routh–Hurwitz conditions on the S–I–R linearization, the time derivative of this Lyapunov function along the solutions is negative definite in a neighbourhood of E^*, which implies the local asymptotic stability of the interior equilibrium.

Introduce the deviations

$$s := S - S^*, \qquad i := I - I^*, \qquad r := R - R^*, \qquad y := x - x^*,$$

and let $z = (s, i, r, y)$. We construct a Lyapunov function of Volterra type for (S, I, R) together with a quadratic term in x.

Define

$$V_1(S, I, R) := \left(S - S^* - S^* \ln \tfrac{S}{S^*}\right) + \left(I - I^* - I^* \ln \tfrac{I}{I^*}\right) + \frac{\delta}{\gamma}\left(R - R^* - R^* \ln \tfrac{R}{R^*}\right),$$

and, for a constant $c > 0$ to be chosen later

$$V(S, I, R, x) := V_1(S, I, R) + c\, y^2.$$

By the convexity of the function $u \mapsto u - u^* - u^* \ln(u/u^*)$, V_1 is C^2 near (S^*, I^*, R^*), vanishes at the equilibrium and is positive definite. Hence, the constants $m_1, m_2 > 0$ and a radius $\rho_0 > 0$ exist such that

$$m_1 \|(s, i, r)\|^2 \le V_1(S, I, R) \le m_2 \|(s, i, r)\|^2 \qquad \text{whenever } \|(s, i, r)\| \le \rho_0.$$

Differentiating V_1 the solutions of (1.2) and using the equilibrium relations (i.e. substituting the right-hand sides and subtracting the linear part at E^*), one obtains the standard decomposition

$$\dot{V}_1 = -Q(s, i, r) + i\, \Phi(i, y),$$

where

- $Q(s, i, r)$ is a quadratic form in (s, i, r), given by

  $$Q(s, i, r) = (s, i, r)\, M\, (s, i, r)^\top,$$

  with M begin equal to the symmetric part of the $S-I-R$ linearization weighted by the Hessian of V_1 at E^*;
- $\Phi(i, y)$ is a smooth function collecting the higher-order terms and the coupling with y, with $\Phi(0, 0) = 0$.

Since all eigenvalues of the S–I–R linearization have negative real parts (by Lemma 3.1), the symmetric matrix M is positive definite. Hence, $\lambda_Q > 0$ and $\rho_1 \in (0, \rho_0]$ exist such that

$$Q(s, i, r) \ge \lambda_Q \|(s, i, r)\|^2 \qquad \text{for all } \|(s, i, r)\| \le \rho_1.$$

Moreover, by the smoothness of Φ and the fact that $\Phi(0, 0) = 0$, the constants $C_1 > 0$ and $\rho_2 \in (0, \rho_1]$ exist such that

$$|\Phi(i, y)| \le C_1(|i| + |y|) \qquad \text{whenever } \|(s, i, r, y)\| \le \rho_2.$$

It follows that in this neighborhood

$$i\, \Phi(i, y) \le C_1(i^2 + |i||y|) \le C_1(i^2 + \tfrac{1}{2}(i^2 + y^2)) \le C_2(i^2 + y^2)$$

for some constant $C_2 > 0$.

Next, we estimate the contribution of the x-equation. From

$$\dot{x} = kx(1-x)(-1+\omega I)$$

and the equilibrium condition $-1+\omega I^* = 0$, we obtain

$$\dot{y} = k(x^*+y)(1-x^*-y)\,\omega i.$$

Hence, for $c > 0$

$$\begin{aligned}\frac{\mathrm{d}}{\mathrm{d}t}(cy^2) &= 2c\,y\,\dot{y}\\ &= 2ck\omega\,y(x^*+y)(1-x^*-y)\,i.\end{aligned}$$

Since the function $(x^*+y)(1-x^*-y)$ is smooth and bounded near $y=0$, the constants $C_3 > 0$ and $\rho_3 \in (0,\rho_2]$ such that

$$\left|\tfrac{\mathrm{d}}{\mathrm{d}t}(cy^2)\right| \le 2cC_3|y|\,|i| \le cC_3(i^2+y^2) \qquad \text{for } \|(s,i,r,y)\| \le \rho_3.$$

Combining the estimates above for $\dot{V}_1$ and $\frac{d}{dt}(cy^2)$, we find that for $\|(s,i,r,y)\| \le \rho_3$,

$$\dot{V} = \dot{V}_1 + \frac{\mathrm{d}}{\mathrm{d}t}(cy^2) \le -\lambda_Q\|(s,i,r)\|^2 + C_2(i^2+y^2) + cC_3(i^2+y^2).$$

Thus the constants $C_4 > 0$ and the (possibly smaller) neighborhood radius $\rho \in (0,\rho_3]$ exist such that

$$\dot{V} \le -\lambda_Q\|(s,i,r)\|^2 + C_4(i^2+y^2), \qquad \|z\| \le \rho.$$

Since $i^2 \le \|(s,i,r)\|^2$, by choosing $c > 0$ sufficiently small (and, if needed, reducing ρ), we can ensure that

$$\dot{V} \le -\lambda(\|(s,i,r)\|^2 + y^2) = -\lambda\|z\|^2$$

for some $\lambda > 0$ and all $\|z\| \le \rho$. On the other hand, the bounds on V_1 together with the term cy^2 imply that V is positive definite and radially bounded in this small neighborhood:

$$\tilde{m}_1\|z\|^2 \le V(z) \le \tilde{m}_2\|z\|^2$$

for a suitable $\tilde{m}_1, \tilde{m}_2 > 0$.

Standard Lyapunov theory now yields local asymptotic stability of the equilibrium E^*: there exists a neighbourhood U of E^* such that any solution starting in U remains in U and converges to E^* as $t \to \infty$. □

For the reader's convenience, here we summarize all THE equilibria of System (1.2) together with their existence conditions and a brief biological interpretation. Detailed coordinate formulas are given in Section 3.

Table 2. Existence conditions and biological meaning of the equilibria of System (1.2).

Equilibrium	Existence condition	Biological interpretation
$E_{DF,0}$	Always feasible for $\Lambda > 0, \mu > 0$	Disease-free equilibrium with $I^* = 0$ and $x^* = 0$; no vaccination is adopted and all newborns enter the susceptible class.
$E_{DF,1}$	$\frac{\Lambda}{\mu} \geq \frac{\mu}{\mu+\delta}$ (so that $S^* \geq 0$)	Disease-free equilibrium with $I^* = 0$ and $x^* = 1$; all newborns are vaccinated at birth and enter the immune class.
E_3	Endemic equilibrium with $x^* = 0$ exists iff $I_3^* > 0 \iff R_0 := \frac{\beta\Lambda}{\mu(\mu+\gamma)} > 1$	Endemic equilibrium in the absence of vaccination ($x = 0$); the disease can persist only when the basic reproduction number R_0 exceeds 1.
E_4	Endemic equilibrium with $x^* = 1$ exists if the steady-state components S_4^*, I_4^*, R_4^* determined in Section 3 satisfy $S_4^* > 0, \quad I_4^* > 0, \quad R_4^* > 0.$	Endemic equilibrium with full newborn vaccination ($x = 1$); infection persists at a reduced level despite universal vaccination at birth.
E_5	Interior equilibrium with $0 < x^* < 1$ exists if $I^* = \frac{1}{\omega} > 0, \quad S^* > 0, \quad R^* > 0,$ $0 < x^* < 1,$ where S^*, R^*, x^* are given explicitly in Section 3. These inequalities impose explicit constraints on $(\beta, \gamma, \mu, \delta, \alpha, \omega, \Lambda)$.	Positive interior equilibrium with coexistence of infection and vaccination behaviour ($0 < x^* < 1$); vaccination coverage and infection prevalence co-evolve, and this equilibrium may lose stability via a Hopf bifurcation.

4. Hopf bifurcation

Before presenting the analytical Hopf bifurcation result, we first illustrate the behavior of solutions near the interior equilibrium E^* by numerical simulations. Throughout this section, we regard ω as the bifurcation parameter. For the baseline parameter set listed in Table 1, we compute the interior equilibrium E^* by solving the steady-state equations with MATLAB's `fsolve`, evaluate the Jacobian matrix $J(E^*, \omega)$ symbolically, and track its eigenvalues as ω varies. The critical value $\omega = \omega^*$ at which a complex conjugate pair of eigenvalues crosses the imaginary axis is consistent with the Hopf condition derived in Theorem 4.1.

In addition, we integrate System (1.2) numerically using the stiff solver `ode15s` on a finite time interval (with tolerances `RelTol = 1e-3`, `AbsTol = 1e-6`), starting from the initial data in a neighbourhood of E^*. For a ω slightly larger than ω^*, the time series of $I(t)$ converges to a stable periodic oscillation around E^*, as illustrated in Figure 1, which corroborates the occurrence of a Hopf bifurcation predicted by our theoretical analysis.

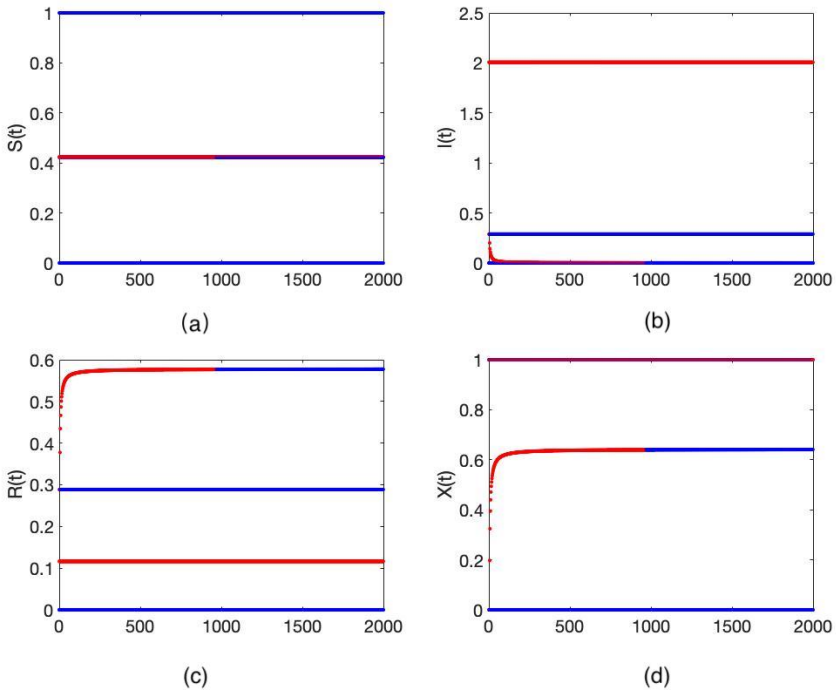

Figure 1. Numerical illustration of a Hopf bifurcation at the interior equilibrium E^* of System (1.2). The plot shows the time evolution of the infectious class $I(t)$ for the baseline parameter set in Table 1, with ω chosen slightly above the critical value ω^* predicted by Theorem 4.1. The system is integrated on the time interval $[0, 100]$ using MATLAB's solver `ode15s` with the tolerances `RelTol = 1e-3`, `AbsTol = 1e-6`, and the initial data taken near E^*. After a transient, the solution converges to a stable periodic orbit, in agreement with the Hopf bifurcation analysis.

In this section, we investigate the existence of a Hopf bifurcation around the positive equilibrium E^* of System (1.2) by taking ω as the bifurcation parameter. On the basis of the general Hopf bifurcation theory of Kuznetsov [24] and the algebraic criterion of Liu [25], we obtain the following result.

Lemma 4.1 (Existence and uniqueness of an interior equilibrium)**.** *Assume that all parameters of System* (1.2) *are strictly positive. Then System* (1.2) *admits* at most one *interior equilibrium*

$$E^* = (S^*, I^*, R^*, x^*) \quad \textit{with} \quad S^*, I^*, R^* > 0,\ 0 < x^* < 1.$$

Moreover, such an interior equilibrium exists if and only if the unique value x^* obtained from the equilibrium equations in Section 2 (case $I^* = 1/\omega$) satisfies $0 < x^* < 1$ and the associated

$$I^* = \frac{1}{\omega}, \qquad S^* = \frac{\mu + \gamma}{\beta}(1 + \alpha I^*), \qquad R^* = \frac{\gamma I^* + \mu x^*}{\mu + \delta}$$

is positive, i.e, $R^* > 0$.

Proof. The equilibrium equations of System (1.2) are solved explicitly in Section 2; in particular, see the paragraph "Interior endemic with $I^* = 1/\omega$ and $x^* \in (0, 1)$" in the subsection on the equilibria of System (1.2).

In that case, the fourth equation of (1.2) implies

$$-1 + \omega I^* = 0 \quad \Longrightarrow \quad I^* = \frac{1}{\omega}.$$

The second equation then gives

$$S^* = \frac{\mu + \gamma}{\beta}(1 + \alpha I^*).$$

The third equation yields

$$R^* = \frac{\gamma I^* + \mu x^*}{\mu + \delta},$$

and the first equation reduces to a *linear* equation in x^* with a unique solution. This shows that, for fixed parameters, there is at most one quadruple (S^*, I^*, R^*, x^*) with $S^*, I^*, R^* > 0$ and $0 < x^* < 1$, i.e. at most one interior equilibrium.

The admissibility conditions $0 < x^* < 1$ and $R^* > 0$ are exactly the positivity requirements on this unique solution. Hence, an interior equilibrium exists if and only if these inequalities are satisfied. This proves the lemma. □

Theorem 4.1. *Consider System* (1.2) *and assume that it admits a positive interior equilibrium*

$$E^* = (S^*, I^*, R^*, x^*), \qquad I^* = \tfrac{1}{\omega},\ 0 < x^* < 1.$$

Let $J(\omega)$ *denote the Jacobian matrix of System* (1.2) *at* E^* *and let*

$$\begin{aligned} p(\lambda, \omega) &= \det\left(\lambda I - J(\omega)\right) \\ &= \lambda^4 + D_1(\omega)\lambda^3 + D_2(\omega)\lambda^2 + D_3(\omega)\lambda + D_4(\omega) \end{aligned}$$

be its characteristic polynomial, where for $j = 1, 2, 3, 4$ *the functions* $D_j(\omega)$ *denote the real-valued coefficient functions of* $p(\cdot, \omega)$*, obtained by expanding* $\det(\lambda I - J(\omega))$*. For convenience, set*

$$D_j'(\omega) = \tfrac{dD_j}{d\omega}$$

and define

$$\Phi(\omega) := D_3(\omega)^2 - D_1(\omega)D_2(\omega)D_3(\omega) + D_1(\omega)^2 D_4(\omega),$$

$$\Psi(\omega) := -D_1^3 D_4' + D_1^2 D_2 D_3' + D_1^2 D_2' D_3 - D_1 D_1' D_2 D_3 - 2D_1 D_3 D_3' + 2D_1' D_3^2,$$

where each D_j, D_j' *is evaluated at the corresponding value of* ω*.*

Assume that $\omega^* > 0$ *exists such that*

*(i) (**Purely imaginary roots**)*

$$\Phi(\omega^*) = 0, \qquad D_1(\omega^*) \neq 0, \qquad \frac{D_3(\omega^*)}{D_1(\omega^*)} > 0.$$

Then one can define

$$\nu^* := \sqrt{\frac{D_3(\omega^*)}{D_1(\omega^*)}} > 0,$$

and $p(\lambda, \omega^*)$ has a pair of simple purely imaginary roots $\lambda = \pm i\nu^*$.

(ii) (***Spectral separation***) *The other two roots of $p(\lambda, \omega^*)$ have nonzero real parts.*

(iii) (***Transversality***)

$$\Psi(\omega^*) \neq 0,$$

which is equivalent to

$$\Re\Big(- \tfrac{p_\omega(i\nu^*, \omega^*)}{p_\lambda(i\nu^*, \omega^*)} \Big) \neq 0,$$

where $p_\lambda := \partial p/\partial\lambda$ and $p_\omega := \partial p/\partial\omega$.

Then, as the parameter ω passes through ω^*, System (1.2) *undergoes a simple Hopf bifurcation at E^*. More precisely, $\varepsilon > 0$ and a smooth family of nontrivial periodic solutions $\Gamma(\omega)$ of System* (1.2) *for $\omega \in (\omega^* - \varepsilon, \omega^* + \varepsilon)$ exist, such that $\Gamma(\omega)$ bifurcates from E^* and its minimal period $T(\omega)$ satisfies*

$$\lim_{\omega \to \omega^*} T(\omega) = \frac{2\pi}{\nu^*}.$$

Moreover, the stability of E^* changes as ω crosses ω^*.

Proof. The Jacobian matrix of System (1.2) at E^* has the form

$$J(\omega) = \begin{pmatrix} d_{11} & d_{12} & \delta & -\mu \\ d_{21} & d_{22} & 0 & 0 \\ 0 & \gamma & d_{33} & \mu \\ 0 & d_{42} & 0 & 0 \end{pmatrix},$$

with the entries

$$\begin{aligned} d_{11} &= -\mu - \frac{\beta}{\omega + \alpha}, & d_{12} &= -\frac{\omega(\mu + \gamma)}{\omega + \alpha}, \\ d_{21} &= \frac{\beta}{\omega + \alpha}, & d_{22} &= -\frac{\alpha(\mu + \gamma)}{\omega + \alpha}, \\ d_{33} &= -(\mu + \delta), & d_{42} &= \omega k x^*(1 - x^*). \end{aligned}$$

Its characteristic polynomial is

$$p(\lambda, \omega) = \lambda^4 + D_1(\omega)\lambda^3 + D_2(\omega)\lambda^2 + D_3(\omega)\lambda + D_4(\omega),$$

where the coefficients $D_j(\omega)$ are expressed in terms of d_{ij} by the usual principal-minor formulas (their explicit expressions are not needed here, except through D_j and D_j').

Step 1: Purely imaginary roots and the function Φ. Assume that, for some ω, $p(\lambda, \omega)$ has a pair of purely imaginary roots $\lambda = \pm i\nu$ with $\nu > 0$. Substituting $\lambda = i\nu$ into $p(\lambda, \omega)$ and separating real and imaginary parts, one obtains the real system

$$\begin{cases} \nu^4 - D_2\nu^2 + D_4 = 0, \\ -D_1\nu^3 + D_3\nu = 0. \end{cases}$$

For $\nu \neq 0$, the second equation yields

$$\nu^2 = \frac{D_3}{D_1}, \qquad D_1 \neq 0.$$

Substituting this into the first equation and multiplying by D_1^2 leads exactly to

$$\Phi(\omega) = D_3^2 - D_1 D_2 D_3 + D_1^2 D_4 = 0.$$

Thus, the condition $\Phi(\omega^*) = 0$, together with $D_1(\omega^*) \neq 0$ and

$$\tfrac{D_3(\omega^*)}{D_1(\omega^*)} > 0,$$

is equivalent to the existence of a pair of purely imaginary roots $\lambda = \pm i\nu^*$ with

$$\nu^* = \sqrt{\frac{D_3(\omega^*)}{D_1(\omega^*)}} > 0.$$

Step 2: Simplicity and transversality. A direct differentiation gives

$$p_\lambda(\lambda, \omega) = 4\lambda^3 + 3D_1\lambda^2 + 2D_2\lambda + D_3,$$
$$p_\omega(\lambda, \omega) = D_1'\lambda^3 + D_2'\lambda^2 + D_3'\lambda + D_4'.$$

Evaluating p_λ at $\lambda = i\nu^*$ and using the relations above, one finds that $p_\lambda(i\nu^*, \omega^*) \neq 0$, so the roots $\pm i\nu^*$ are simple.

Differentiating the root relation $p(\lambda(\omega), \omega) = 0$ with respect to ω gives

$$\frac{\mathrm{d}\lambda}{\mathrm{d}\omega}\Big|_{\omega=\omega^*} = -\frac{p_\omega(i\nu^*, \omega^*)}{p_\lambda(i\nu^*, \omega^*)}.$$

A straightforward (though tedious) computation shows that

$$\Re\Big(-\frac{p_\omega(i\nu^*, \omega^*)}{p_\lambda(i\nu^*, \omega^*)}\Big) = C(\omega^*)\,\Psi(\omega^*),$$

where $C(\omega^*) \neq 0$ is an explicit nonzero factor depending on $D_1(\omega^*), D_3(\omega^*)$. Hence the transversality condition

$$\Re\Big(-\frac{p_\omega(i\nu^*, \omega^*)}{p_\lambda(i\nu^*, \omega^*)}\Big) \neq 0$$

is equivalent to $\Psi(\omega^*) \neq 0$. This proves that as ω passes through ω^*, the simple pair of eigenvalues $\lambda(\omega), \overline{\lambda(\omega)}$ crosses the imaginary axis with nonzero speed, while, by Assumption (ii), the remaining two eigenvalues never lie on the imaginary axis.

Step 3: Application of the Hopf bifurcation theorem and the period. By the classical Hopf bifurcation theorem (see, e.g., Hassard et al. [26] and Kuznetsov [27]), Hypotheses (i)–(iii) imply that System (1.2) undergoes a simple Hopf bifurcation at $\omega = \omega^*$: We then have $\varepsilon > 0$ and a smooth family of nontrivial periodic solutions $\Gamma(\omega)$ bifurcating from E^* for $\omega \in (\omega^* - \varepsilon, \omega^* + \varepsilon)$, and their minimal period $T(\omega)$ satisfies

$$T(\omega) = \frac{2\pi}{|\Im\,\lambda(\omega)|} + o(1) \quad \text{as } \omega \to \omega^*,$$

where $\lambda(\omega)$ is the eigenvalue branch with $\lambda(\omega^*) = i\nu^*$. In particular

$$\lim_{\omega\to\omega^*} T(\omega) = \frac{2\pi}{\nu^*}.$$

Moreover, the change of sign of $\Re\,\lambda(\omega)$ implied by (iii) guarantees that the stability of E^* changes when ω crosses ω^*. This completes the proof. □

5. Numerical simulations

All numerical experiments in this section were carried out in `MATLAB R2018a` (MathWorks, Natick, MA, USA) on a 64-bit `macOS` system. For the simulation of System (1.2), we used the variable-step stiff ODE solver `ode15s` over the time interval $[0, 100]$, with the outputs recorded at integer time points. Unless otherwise stated, the default MATLAB error tolerances (`RelTol = 1e-3`, `AbsTol = 1e-6`) were employed. For the global sensitivity analysis based on partial rank correlation coefficients (PRCCs), we generated $N = 1000$ Latin hypercube samples over the parameter ranges listed in Table 3 and computed PRCC values using a MATLAB implementation of the algorithm by Marino et al. [28].

Table 3. Parameter ranges used for the sensitivity analysis of System (1.2).

Parameter	Baseline	Minimum	Maximum
β	0.9	0.7585	0.9633
γ	0.2	0.1608	0.2398
k	0.002	0.0015	0.0023
μ	0.18	0.1381	0.2103
α	0.004	0.0031	0.0052
ω	100	75.473	119.6882

To determine which parameters significantly influence the infectious population in System (1.2), we conduct a global sensitivity analysis using the PRCC method. Sensitivity analysis based on PRCC and Latin hypercube sampling has been widely used in systems biology and ecological/epidemiological modeling; see, for example, Marino et al. [28] and Imron et al. [29]. Since the relationships between the model's inputs and outputs are assumed to be nonlinear yet monotonic, the PRCC method is well-suited for this setting. To implement it, we perform Latin hypercube sampling based on the baseline parameter ranges specified in Table 3, generating $N = 1000$ independent simulation samples. For each sample, we numerically integrate System (1.2) on the time interval $[0, 100]$ with fixed initial conditions (as specified below in this section) and use the resulting trajectories to compute the PRCC values at selected time points. The corresponding numerical results are summarized in Figures 2 and 3.

Choice of parameter bounds in Table 3. The baseline values in Table 3 coincide with the parameter set used in the qualitative analysis of equilibria and Hopf-type dynamics in Sections 3 and 4, for which the model admits a biologically meaningful interior equilibrium.

The lower and upper bounds were chosen as moderate perturbations around these baseline values, guided by two criteria: (i) Biological plausibility of the corresponding time scales (infection,

recovery, waning immunity, and natural mortality), and (ii) numerical simulations indicating that, throughout the chosen ranges, all state variables remain non-negative and bounded and the system stays in a qualitatively similar dynamic regime (the existence of an interior equilibrium with possible oscillations). Concretely, for each parameter, we varied its value by roughly 10–20% around the baseline, performed test simulations of System (1.2) on the time interval $[0, 100]$, and restricted the admissible interval to the region where the solutions remained epidemiologically meaningful. The final minimum and maximum values reported in Table 3 are the endpoints of these numerically validated intervals.

On the basis of these samples, we obtain an ensemble of infectious trajectories $I(t)$, which visualizes the spread of the epidemic's outcomes under parameter uncertainty. These ensemble trajectories and the associated parameter–output relationships provide the basis for the PRCC computations. Together, Figures 2 and 3 summarize the pathway from parameter uncertainty to an ensemble of epidemic trajectories and then to parameter–output relationships, which form the basis for the PRCC-based global sensitivity analysis.

Stability and Hopf bifurcation. We now analyze the stability behavior of System (1.2), assuming the initial conditions $S(0) = 0.6$, $I(0) = 0.1$, $R(0) = 0.2$, and $x(0) = 0.2$. From Theorems 2.4 and 2.5, the local asymptotic stability of the equilibria E_3 and E_4 is confirmed. In addition, Theorem 3.1 shows that System (1.2) admits a positive equilibrium E_5. Using the parameter set $\gamma = 0.2$, $\delta = 0.02$, $\mu = 0.18$, $\alpha = 0.004$, $\beta = 0.9$, and $k = 0.002$ and varying the behavioral sensitivity parameter ω, we integrate System (1.2) on the time interval $[0, 100]$ with the initial conditions $S(0) = 0.6$, $I(0) = 0.1$, $R(0) = 0.2$, $x(0) = 0.2$, and observe that a supercritical Hopf bifurcation occurs at $\omega = 1000$. In the following simulations, we therefore set $\omega = 1000$ to illustrate a high-sensitivity regime in which behavioural feedback is strong enough to trigger a Hopf bifurcation. The corresponding numerical simulations are summarized in Figure 4.

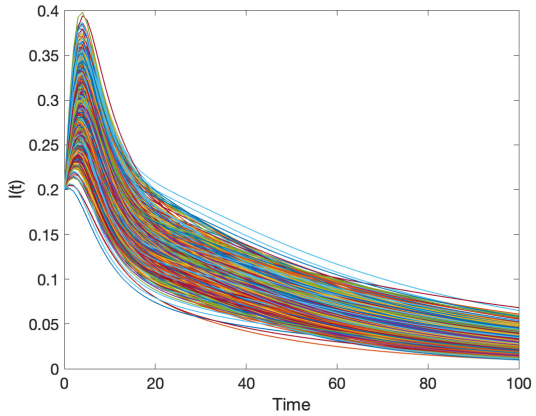

Figure 2. Ensemble of infected individuals $I(t)$ for $N = 1000$ Latin Hypercube samples of the parameters in System (1.2). Each thin curve represents the infectious population $I(t)$ over the time interval $[0, 100]$ for one parameter sample drawn from the ranges in Table 3, starting from fixed initial conditions (see Section 5). The bundle of trajectories illustrates the variability in epidemic outcomes induced by parameter uncertainty.

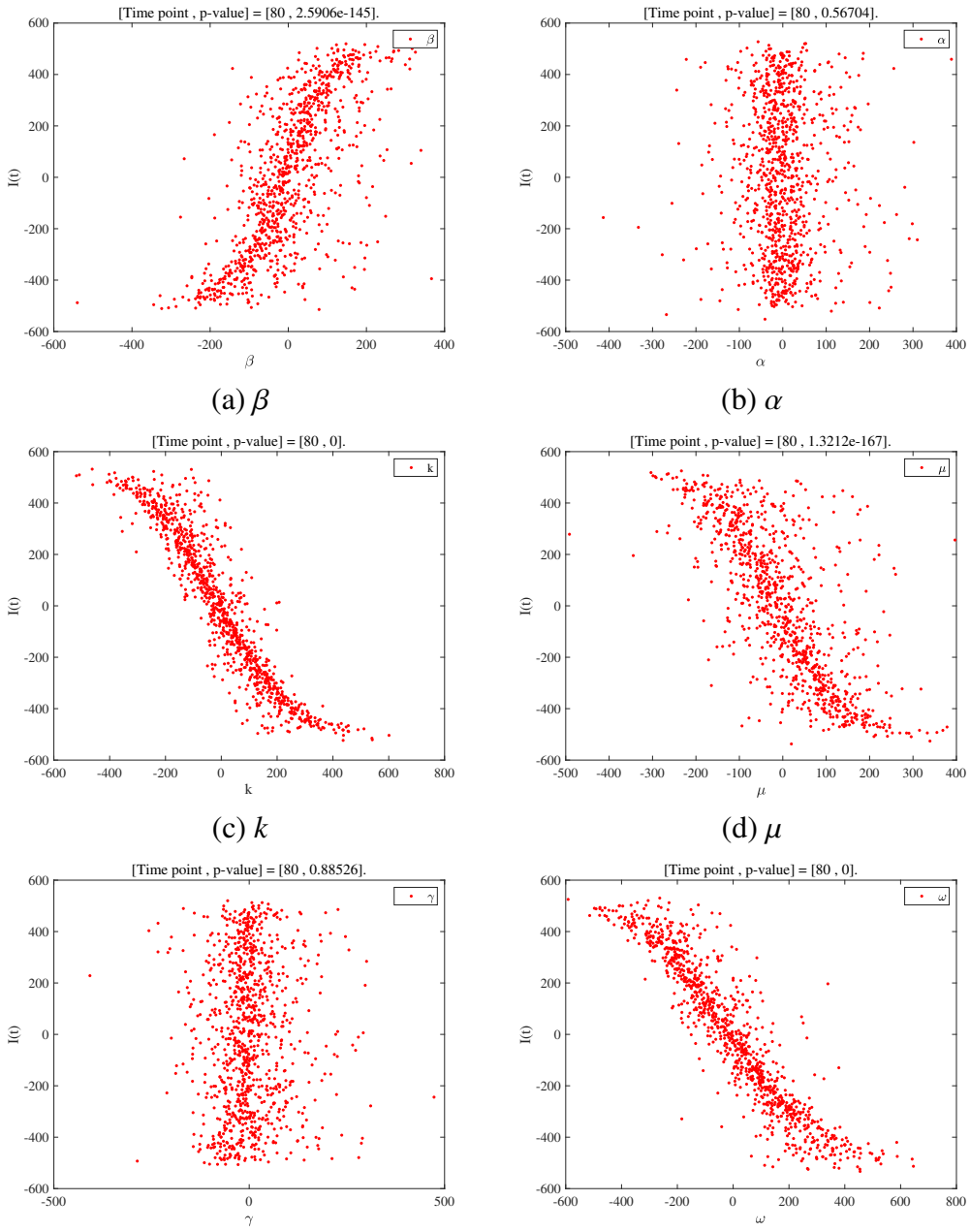

Figure 3. Scatter plots showing the relationship between the infectious population $I(t)$ and the sampled parameters in System (1.2). Each panel compares $I(t)$ (evaluated at a representative later time during the simulation) with one of the parameters from Table 3. The approximately monotonic positive or negative trends observed in these plots support the use of PRCC as a global sensitivity measure for this model. In particular, for the behavioural parameters k and ω, the scatter plots indicate that increasing these parameters can substantially modify the amplitude and spread of the infectious trajectories, reflecting how imitation dynamics and risk sensitivity amplify or attenuate the epidemic burden.

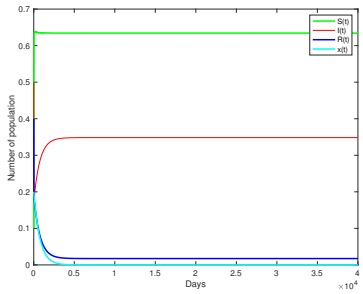

(a) Time series converging to E_3 (no vaccination).

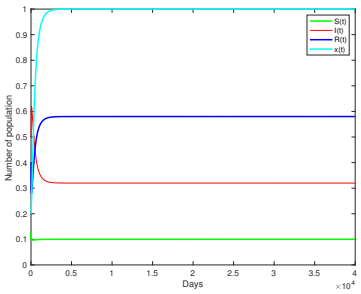

(b) Time series converging to E_4 (full vaccination).

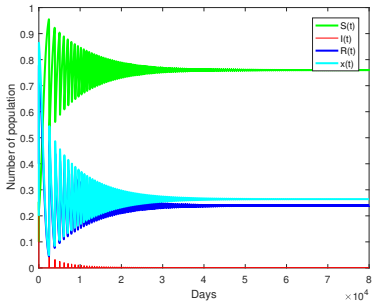

(c) Time series approaching E_5 for $\omega < \omega^*$.

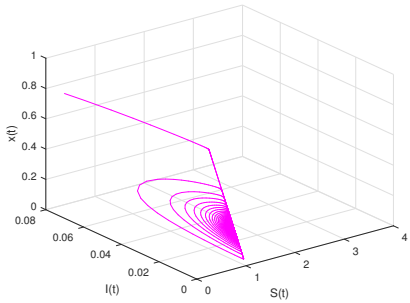

(d) Phase portrait near E_5 for $\omega < \omega^*$.

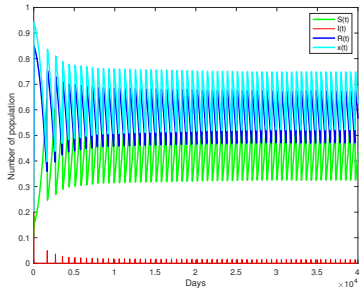

(e) Sustained oscillations in $I(t)$ and $x(t)$ for $\omega > \omega^* = 1000$.

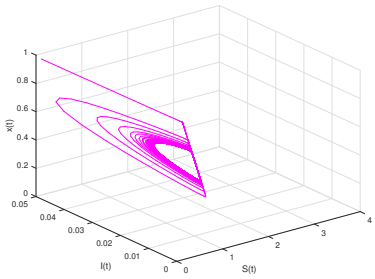

(f) Limit cycle in the (I, x)–plane after Hopf bifurcation.

Figure 4. Numerical simulations illustrating the stability of the boundary equilibria E_3 and E_4 and the interior equilibrium E_5, as well as the emergence of a Hopf bifurcation in System (1.2). Panels (a) and (b) show the time evolution of the epidemiological variables when the boundary endemic equilibria E_3 (no vaccination) and E_4 (full vaccination) are locally asymptotically stable. Panels (c) and (d) present the time series and phase portrait corresponding to the positive interior equilibrium E_5 for ω below the Hopf threshold ω^*. Panels (e) and (f) display the sustained oscillations and the associated limit cycle in the (I, x)-plane that arise after the supercritical Hopf bifurcation at $\omega = 1000$. In all panels, the horizontal axis represents time t (in days) for the time-series plots, and the vertical axes denote the fractions of the corresponding compartments. All simulations are performed with the parameter values given in Section 5 and initial conditions $S(0) = 0.6$, $I(0) = 0.1$, $R(0) = 0.2$ and $x(0) = 0.2$.

6. Conclusions

In this work, we have developed and analyzed an SIR epidemic model that incorporates adaptive vaccination behavior through a game-theoretic imitation mechanism. By coupling classical disease dynamics with behavioral dynamics, our model captures how individuals' risk perception and social influence jointly shape vaccination coverage and, in turn, disease prevalence. We provided a rigorous mathematical analysis of the equilibria and their local stability, identified the conditions under which Hopf bifurcation may occur, and revealed the possibility of sustained oscillations emerging from the interaction between epidemiological and behavioral processes.

The main contribution of this study lies in integrating realistic human decision-making into the epidemic modeling framework in a mathematically tractable way. Compared with traditional models that treat vaccination as a constant-rate intervention, our approach highlights how strategic decision-making may produce nontrivial dynamic outcomes such as oscillations and bistability. These findings provide theoretical insights into the design of vaccination strategies, suggesting that policies should not only focus on biological control parameters but also account for the adaptive nature of human behavior (e.g, through risk communication, reductions in the perceived vaccine risk, and stabilization of vaccination coverage). In particular, our analysis shows that higher perceived vaccine risk can push the system from a disease-control regime to persistent endemicity, while increasing the behavioral sensitivity ω may destabilize an otherwise stable endemic equilibrium and trigger Hopf bifurcation, leading to recurrent epidemic oscillations.

From a biological and public health viewpoint, these Hopf bifurcations correspond to the onset of sustained epidemic oscillations driven by behavioral feedback between vaccination coverage and disease prevalence. When the prevalence $I(t)$ is low, individuals perceive a low infection risk, vaccination willingness $x(t)$ decreases, and overall coverage gradually declines, which allows the disease to resurge. As $I(t)$ increases again, the perceived infection risk becomes more salient, imitation dynamics promote higher vaccination uptake among parents, and the system is pushed back toward disease control. Once the endemic equilibrium loses stability through a Hopf bifurcation, this negative feedback loop between risk perception, imitation-based vaccination, and disease transmission can sustain recurrent epidemic waves *without* any external forcing (such as seasonality), providing a mechanism for endogenous, behavior-driven epidemic cycles.

Beyond these qualitative mechanisms, our analysis also clarifies how key parameters shape the overall dynamic behavior. The behavioural sensitivity ω acts as a primary bifurcation parameter: Increasing ω can destabilize an otherwise stable endemic equilibrium and give rise to sustained oscillations. The waning immunity rate δ controls how rapidly recovered individuals return to the susceptible class, thereby modulating both the endemic level of infection and the likelihood of recurrent outbreaks. The saturation parameter α weakens transmission at high prevalence, altering the location and stability of endemic equilibria by limiting the effective force of infection. Finally, the imitation rate k governs the speed of behavioral adjustment, influencing how quickly vaccination coverage responds to changes in the disease's prevalence and thus affecting the transient approach to equilibrium or to a limit cycle.

From a modeling perspective, our framework generalizes several classical SIR-type formulations. In particular, we qualitatively compared our results with (i) models with bilinear incidence and no waning immunity, (ii) models with waning immunity but without imitation-based vaccination, and

(iii) models with behavioral or information-dependent vaccination but without saturated incidence or $R \to S$ transitions. This comparison shows that the simultaneous inclusion of saturated incidence, waning immunity, and imitation dynamics can change the number and type of equilibria, alter the onset of Hopf bifurcation, and generate endogenous oscillations that do not appear in simpler models.

Despite these advantages, the present study also has several limitations. First, key behavioral parameters (such as the sensitivity of perceived risk to prevalence) are phenomenological and are not directly measurable in practice. Second, the model assumes homogeneous mixing and symmetric behavior across individuals, so heterogeneity in age, risk perception, socioeconomic status, or access to vaccination is not captured. Third, spatial structure, contact networks, and other forms of population heterogeneity are not explicitly modeled. These limitations mean that the quantitative predictions of the model should be interpreted with caution, while the qualitative mechanisms remain informative.

From the viewpoint of stochastic effects, we also note that our analysis is based on a deterministic SIR-imitation framework. In realistic settings, however, demographic noise, random variation in contact patterns, and abrupt changes in risk perception may play a non-negligible role. A natural extension of the present work would therefore be to formulate stochastic versions of the model, for example, by introducing stochastic differential equations with noise terms in the infection or imitation dynamics, or by constructing Markov chain and agent-based formulations in which the vaccination game is played at the level of discrete individuals. A systematic investigation of such stochastic extensions lies beyond the scope of this paper and is left as an interesting direction for future research.

Future work may extend the current framework along several directions. For clarity, here we summarize a few concrete lines of further research.

- **Heterogeneous populations:** Incorporate multiple behavioral or demographic classes (e.g, different age groups, risk perceptions, or vaccine access levels) to study how heterogeneity modifies the imitation dynamics and the resulting epidemic outcomes.
- **Network- and space-structured transmission:** Replace the homogeneous mixing assumption with spatial or network-based contact structures, and investigate how local clustering and community structure affect behavior-driven oscillations and bifurcations.
- **Richer payoff and behavioral rules:** Consider more detailed psychological or economic payoff structures, bounded rationality, information delays, and media- or platform-driven changes in perceived infection and vaccine risks.
- **Stochastic extensions:** Develop stochastic counterparts of the present model (stochastic differential equations (SDEs), Markov chain models, or agent-based formulations) to quantify the impact of demographic and behavioral noise, especially near Hopf bifurcation thresholds.
- **Empirical data and calibration:** Collect empirical data on perceived infection risk, vaccine risk, and imitation strength among vaccinated and unvaccinated individuals, and use such data to calibrate the behavioral parameters and validate the qualitative mechanisms identified here.

These directions would further enhance the predictive and explanatory power of the model and help bridge the gap between theoretical behavior–epidemic coupling and real-world vaccination policy design.

Author contributions

Fengjun Li: Conceptualization, Methodology, Formal analysis, Writing-original draft; Tao Zhang: Numerical simulations, Investigation, Writing-review and editing; Qimin Zhang: Model validation, Visualization, Writing-review and editing. All authors have read and approved the final version of the manuscript for publication.

Use of Generative-AI tools declaration

The authors declare that they have not used Artificial Intelligence (AI) tools in the creation of this article.

Conflict of interest

The authors declare no conflicts of interest.

References

1. A. N. Ifati, R. Herdiana, R. H. Utomo, A. H. Permatasari, Analysis of a mathematical model in the spread of tuberculosis epidemic with vaccination and relapse effect, *J. Phys.: Conf. Ser.*, **1943** (2021), 012131. http://doi.org/10.1088/1742-6596/1943/1/012131
2. X. Wang, J. Li, J. Liu, X. Wu, Dynamical vaccination behavior with risk perception and vaccination rewards, *Chaos*, **34** (2024), 033109. https://doi.org/10.1063/5.0186899
3. S. Mungkasi, Variational iteration and successive approximation methods for an SIR epidemic model with constant vaccination strategy, *Appl. Math. Model.*, **90** (2021), 1–10. https://doi.org/10.1016/j.apm.2020.08.058
4. K. H. Lavail, A. M. Kennedy, The role of attitudes about vaccine safety, efficacy, and value in explaining parents' reported vaccination behavior, *Health Educ. Behav.*, **40** (2013), 544–551. https://doi.org/10.1177/1090198112463022
5. X. Chen, F. Fu, Imperfect vaccine and hysteresis, *Proc. Biol. Sci.*, **286** (2019), 20182406. https://doi.org/10.1098/rspb.2018.2406
6. G. Guan, Z. Guo, Y. Xiao, Dynamical behaviors of a network-based SIR epidemic model with saturated incidence and pulse vaccination, *Commun. Nonlinear Sci. Numer. Simul.*, **137** (2024), 108097. https://doi.org/10.1016/j.cnsns.2024.108097
7. F. M. Burkle, Declining public health protections within autocratic regimes: Impact on global public health security, infectious disease outbreaks, epidemics, and pandemics, *Prehosp. Disaster Med.*, **35** (2020), 237–246. https://doi.org/10.1017/S1049023X20000424
8. A. Chhabra, Covid-19 vaccination, *Int. J. Innov. Res. Technol.*, **8** (2021), 1–5.
9. J. Nunuvero, A. Santiago, Modeling the effects of adherence to vaccination and health protocols in epidemic dynamics by means of an SIR model, preprint paper, 2023. https://doi.org/10.48550/arXiv.2308.01038

10. A. Deka, S. Bhattacharyya, The effect of human vaccination behaviour on strain competition in an infectious disease: An imitation dynamic approach, *Theoret. Popul. Biol.*, **143** (2022), 62–76. https://doi.org/10.1016/j.tpb.2021.12.001

11. P. Joe, C. T. Bauch, The influence of social behavior on selection and spread of virulent pathogen strains, *J. Theoret. Biol.*, **455** (2018), 47–53.

12. M. Saade, S. Ghosh, M. Banerjee, V. Volpert, Delay epidemic models determined by latency, infection, and immunity duration, *Math. Biosci.*, **370** (2024), 109155. https://doi.org/10.1016/j.mbs.2024.109155

13. B. Buonomo, A. d'Onofrio, D. Lacitignola, Global stability of an SIR epidemic model with information-dependent vaccination, *Math. Biosci.*, **216** (2008), 9–16. https://doi.org/10.1016/j.mbs.2008.07.011

14. J. Tang, Y. Yao, M. Xie, M. Feng, SIS epidemic modelling on homogeneous networked system: General recovering process and mean-field perspective, *Appl. Math. Model.*, **146** (2025), 116188. https://doi.org/10.1016/j.apm.2025.116188

15. X. Yuan, Y. Yao, X. Li, M. Feng, Impact of time-dependent infection rate and self-isolation awareness on networked epidemic propagation, *Nonlinear Dyn.*, **112** (2024), 15653–15669. https://doi.org/10.1007/s11071-024-09832-0

16. X. Yuan, Y. Yao, H. Wu, M. Feng, Impacts of physical-layer information on epidemic spreading in cyber-physical networked systems, *IEEE Trans. Circuits Syst. I: Regular Papers*, **72** (2025), 5957–5969. https://doi.org/10.1109/TCSI.2025.3550386

17. M. Feng, Z. Zeng, Q. Li, M. Perc, J. Kurths, Information dynamics in evolving networks based on the birth-death process: Random drift and natural selection perspective, *IEEE Trans. Syst. Man Cyber.: Syst.*, **54** (2024), 5123–5136. https://doi.org/10.1109/TSMC.2024.3389095

18. M. Feng, X. Li, Y. Li, Q. Li, The impact of nodes of information dissemination on epidemic spreading in dynamic multiplex networks, *Chaos*, **33** (2023), 043112. https://doi.org/10.1063/5.0142386

19. C. T. Bauch, Imitation dynamics predict vaccinating behaviour, *Proc. Biol. Sci.*, **272** (2005), 1669–1675. https://doi.org/10.1098/rspb.2005.3153

20. J. Hofbauer, K. Sigmund, *Evolutionary Games and Population Dynamics*, Cambridge: Cambridge University Press, 1998.

21. C. T. Bauch, D. J. D. Earn, Vaccination and the theory of games, *Proc. National Acad. Sci. USA*, **101** (2004), 13391–13394. https://doi.org/10.1073/pnas.0403823101

22. R. M. Anderson, R. M. May, *Infectious Diseases of Humans: Dynamics and Control*, Oxford: Oxford University Press, 1991.

23. S. Ruan, W. Wang, Dynamical behavior of an epidemic model with a nonlinear incidence rate, *J. Differ. Equ.*, **188** (2003), 135–163. https://doi.org/10.1016/S0022-0396(02)00089-X

24. Y. A. Kuznetsov, *Elements of Applied Bifurcation Theory*, 2 Eds., New York: Springer, 1998.

25. W. M. Liu, Criterion of Hopf bifurcations without using eigenvalues, *J. Math. Anal. Appl.*, **182** (1994), 250–256. https://doi.org/10.1006/jmaa.1994.1079

26. B. D. Hassard, N. D. Kazarinoff, Y. H. Wan, *Theory and Applications of Hopf Bifurcation*, Cambridge: Cambridge University Press, 1981.

27. Y. A. Kuznetsov, *Elements of Applied Bifurcation Theory*, New York: Springer, 2004.

28. S. Marino, I. B. Hogue, C. J. Ray, D. E. Kirschner, A methodology for performing global uncertainty and sensitivity analysis in systems biology, *J. Theoret. Biol.*, **254** (2008), 178–196. https://doi.org/10.1016/j.jtbi.2008.04.011

29. M. A. Imron, A. Gergs, U. Berger, Structure and sensitivity analysis of individual-based predator–prey models, *Reliab. Eng. Syst. Saf.*, **107** (2012), 71–81. https://doi.org/10.1016/j.ress.2011.07.005

AIMS Press